Physica Scripta. Vol. 43, 137–143, 1991.

# Isoelectronic Smoothing of Line Strengths in Intermediate Coupling

Lorenzo J. Curtis

Department of Physics and Astronomy, University of Toledo, Toledo OH 43606, U.S.A.

*Received August 29, 1990; accepted September 25, 1990*

**Abstract**

A method is presented that accounts for the effects of singlet-triplet mixing in measured lifetimes of resonance and intercombination lines in alkaline-earthlike and inert-gaslike isoelectronic sequences. The method uses measured lifetimes and spectroscopic energy levels as its only inputs, and yields mixing-reduced line strength factors that can be isoelectronically linearized for precision interpolation, extrapolation, and smoothing. The method is applied to predictively systematize lifetimes in the Be, Mg and Ne isoelectronic sequences.

## 1. Introduction

It is well known [1–3] that lifetime measurements for resonance transitions in one and two valence electron ions can be isoelectronically linearized through a reduction to effective line strengths, which are then represented by a screening parametrization. This systematization permits lifetime measurements for different ions in the same isoelectronic sequence to be examined for consistency, to be smoothed to increase the individual accuracies, to be predictively interpolated and extrapolated, and to be sensitively compared with theoretical predictions. In the case of the two valence electron systems, the isoelectronic increase of singlet-triplet mixing arising from intermediate angular momentum coupling is expected to affect these lifetimes at higher ionicities, since this mixing places the resonance and intercombination amplitudes in unitary quadrature.

A method is presented here for accounting for the effects of intermediate coupling on measured lifetimes of both the resonance and intercombination lines. The method is entirely empirical and uses as its only inputs the experimentally determined lifetimes and energy levels. The method is described below, and applied to make predictive empirical lifetime systematizations for ions in the Be, Mg and Ne isoelectronic sequences.

## 2. Computational formulation

A traditional way of presenting measured atomic lifetime and transition probability data is through exposition on a plot of the absorption oscillator strength $f$ vs the reciprocal of the nuclear charge $Z$. Although this exposition employs a physically meaningful quantity $f$ as its ordinate, such plots are usually not monotonic for resonance transitions in which the principal quantum number $n$ does not change. It has been shown [1–3] that a monotonic, regular and nearly linear plot can be obtained if lifetime data are instead reduced to line strengths $S$, related to measured quantities for an unbranched decay by

$$S = [\lambda(\text{Å})/1265.38]^3(2J + 1)/\tau(\text{ns}), \quad (1)$$

where $J$ and $\tau$ are the total angular momentum and lifetime of the upper level, and $\lambda$ is the transition wavelength. References [1–3] have demonstrated that values of $S$ for some isoelectronic sequences can be accurately represented by a semiempirical screening parameter linearization of the form

$$Z^2S = A + B/(Z - C). \quad (2)$$

Higher order corrections in powers of the reciprocal screened charge have sometimes been included [2, 3] to improve interpolative accuracy, but these can introduce distortions if extrapolations are attempted. In the considerations that follow, eq. (2) will be adopted as an approximate method for parametrizing existing data, with the anticipation that improved parametrizations can be used as precision lifetime measurements at higher $Z$ become available.

Figure 1 presents an exposition of measured lifetime data [4] reduced to values for $Z^2S$ (denoted by circles) for the $3s\ ^2S_{1/2}$–$3p\ ^2P_J$ transitions in the Na isoelectronic sequence. Here no attempt has been made to optimize the linearity by adjusting $C$, and a value $C = 10$ was used to represent the limit of complete screening by the core electrons. Notice that the $J = 1/2$ and $3/2$ levels have different slopes and intercepts on this plot, but both are well represented by eq. (2). Also shown in Fig. 1 are the published results of an *ab initio* calculation [5] (dashed lines) and a model potential quantum defect computation [4] (solid lines). Figure 1 clearly illustrates the power of this exposition to verify the validity of isoelectronic sets of experimental data, to improve the individual accuracies by isoelectronic smoothing, and to comparatively evaluate various theoretical approaches.

Successful parametrizations [2, 3] have also been made of existing measured lifetime data for the $2s^2\ ^1S_0$–$2s2p\ ^1P_1$ transitions in the Be isoelectronic sequence. In this two valence electron case, the presence of a core electron with the same value of $n$ as the active electron leads to partial core screening, and the quantity $C$ in eq. (2) is usually treated as a third adjustable fitting parameter. Although the fits presented in Refs. [2, 3] adequately describe the moderate stages of ionization for which measurements presently exist, it is expected that for sufficiently high $Z$ this transition rate will be partially channelled through its mixing partner, the $2s^2\ ^1S_0$–$2s2p\ ^3P_1$ transition. Since these spin designations are only nominal in the presence of intermediate coupling, the physical states will henceforth be denoted by $^1P_1'$ and $^3P_1'$, using primes to differentiate them from the pure $LS$ basis states.

We have recently formulated a procedure [6] for specifying these intermediate coupling effects using measured energy level data. This procedure can be applied here to extend the

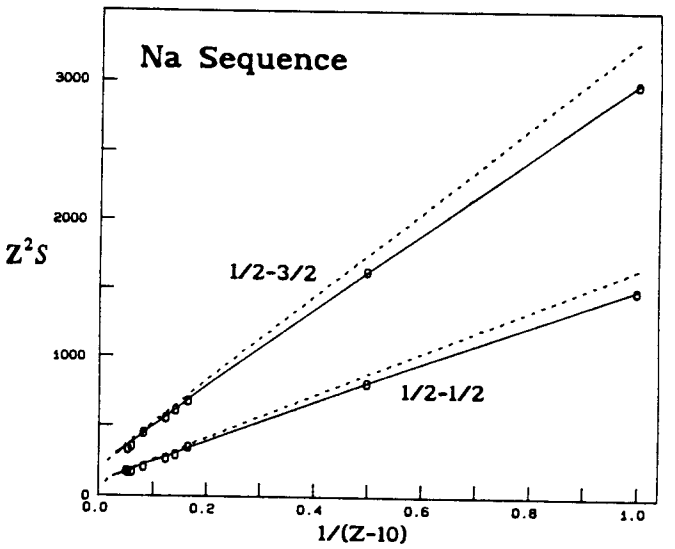


*Fig. 1.* Lifetimes for the $3s$–$3p$ resonance transitions in the Na isoelectronic sequence, converted to the line strength factors $Z^2S$, vs the reciprocal screened central charge $1/(Z\text{-}10)$. Experimental measurements are denoted by (0), solid lines indicate semiempirical calculations [4], and dashed lines indicate *ab initio* MCDF calculations [5].

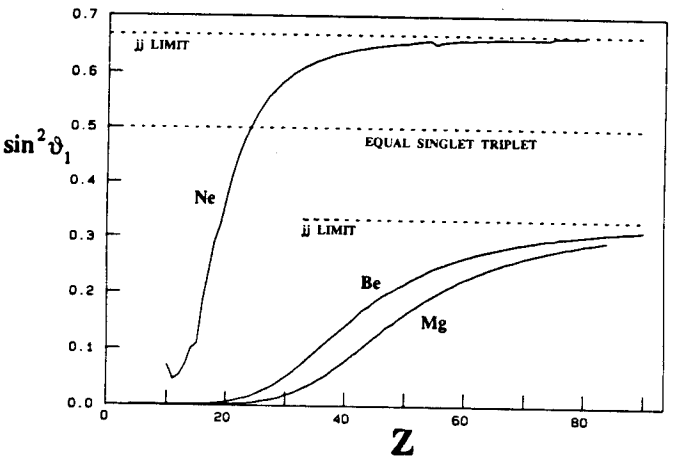


*Fig. 2.* Plot of the singlet-triplet mixing fraction $\sin^2\theta_1$, determined from spectroscopic energy level data for the Be [19–22], Mg [39–46] and Ne [51–59] isoelectronic sequences, vs. the nuclear charge $Z$.

methods of Refs. [2, 3] to high $Z$ and to include both the intercombination and resonance transition lifetimes.

For systems with two out-of-shell electrons, singlet-triplet and $L$-state mixing within a given configuration manifests itself in the energy splittings and line strengths of the constituent levels. In intermediate coupling, the wave functions of levels with the same $J$ and parent configuration are an admixture of $LS$ basis states that is not subject to the $\Delta L$ and $\Delta S$ selection rules that restrict the constituent amplitudes. In *ab initio* calculations this is implicitly included in the wave function. It is also possible to empirically determine the mixing amplitudes (within the single configuration approximation) explicitly from energy level data, and to semiempirically specify the effective radial transition moments exclusive of the angular momentum coupling.

The $nsn'l$, $nsn'p^5$, $np^2$ and $np^4$ configurations present particularly simple examples of intermediate coupling, since they contain no more than two levels of the same $J$, so that the spin–orbit interaction connects the $LS$ basis states only pairwise. The $LS$ specification involves a $2 \times 2$ nondiagonal matrix $\boldsymbol{M}$ and diagonalization is achieved by a basis transformation $\boldsymbol{T}^{-1}\boldsymbol{M}\boldsymbol{T}$, where

$$\boldsymbol{T} = \begin{pmatrix} \cos\theta_J & \sin\theta_J \\ -\sin\theta_J & \cos\theta_J \end{pmatrix}. \tag{3}$$

Here the normalized amplitudes can be described by a single quantity $\theta_J$, the abstract singlet-triplet mixing angle. This can be written as

$$\cos(2\theta_J) \equiv \pm W_J/\sqrt{1 + W_J^2}, \tag{4}$$

where the quantity $W_J$ is proportional to the ratio of the electrostatic and spin–orbit Slater energies, and can be conveniently expressed in terms of the $J$ centroid energies $\varepsilon_J$ of the levels within the configuration. For the $nsn'p$ and $np^5n's$ configurations, only the $J = 1$ levels are mixed and $W_1$ is given by

$$W_1 = [3(\varepsilon_1 - \varepsilon_0)/(\varepsilon_2 - \varepsilon_0) - 1]/\sqrt{2}. \tag{5}$$

The sign in eq. (4) is chosen so that $\theta_J$ is small for low $Z$. A plot of $\sin^2\theta_1$ vs. $Z$, obtained from spectroscopic data for the Be, Mg and Ne isoelectronic sequences using eqs. (4, 5), is shown in Fig. 2. Tests of these formulae applied to *ab initio* multiconfiguration theoretical data [6] indicate that the mixing angles thus obtained can be reliable even in cases where the single configuration picture is not strictly valid.

In terms of the $J = 1$ mixing angle, the line strengths for the resonance and intercombination lines in $ns^2$–$nsn'p$ or $n'p^6$–$nsn'p^5$ transitions are

$$S(^1S_0, {}^1P_1') = k\cos^2\theta_1\,|\langle ns|r|n'p0\rangle|^2 \tag{6}$$

$$S(^1S_0, {}^3P_1') = k\sin^2\theta_1\,|\langle ns|r|n'p1\rangle|^2 \tag{7}$$

where the factor $k$ accounts for the number of equivalent electrons and various angular momentum factors. If the measured lifetimes are converted to line strengths using eq. (1), quantities proportional to these squared transition moments can be obtained by dividing out the mixing angle factors. Thus the mixing-reduced effective line strengths $S_r$ are defined as

$$S_r(\text{Res}) \equiv S(^1S_0, {}^1P_1')/\cos^2\theta_1 \tag{8}$$

and

$$S_r(\text{Int}) \equiv S(^1S_0, {}^3P_1')/\sin^2\theta_1. \tag{9}$$

In this way a new empirical exposition equivalent to that shown in Fig. 1 is obtained. Figures 3–5 present predictive expositions of the Be, Mg and Ne isoelectronic sequences.

## 3. The Be isoelectronic sequence

An exposition of the reduction of the $2s^2$–$2s2p$ resonance and intercombination transition lifetime data in the Be sequence to the quantities $Z^2S_r(\text{Res})$ (denoted by 0) and $Z^2S_r(\text{Int})$ (denoted by X) is presented in Fig. 3. Measured lifetime data were obtained from Refs. [7–13] for the resonance lines and from Refs. [14–17] for the intercombination lines. For high $Z$, the experimental lifetime data displayed on this plot have been supplemented by published multiconfiguration Dirac–Fock (MCDF) theoretical calculations [18]. The measured lifetimes and their quoted uncertainties, together with

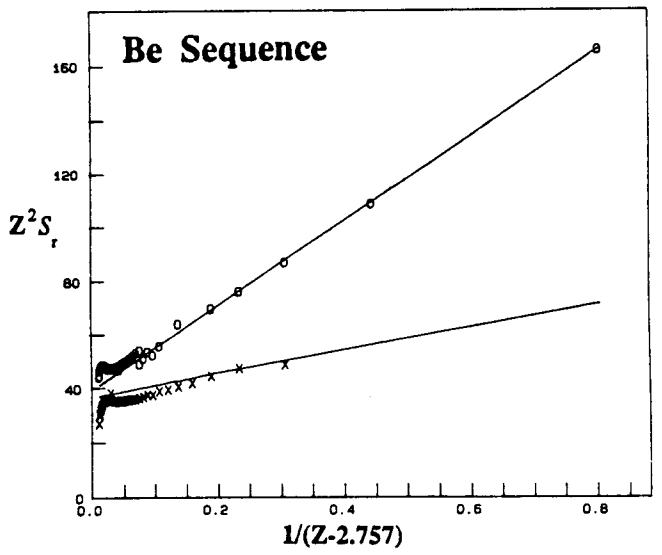


*Fig. 3.* Lifetimes for the $2s^2$–$2s2p$ resonance and intercombination transitions in the Be sequence, converted to spin-mixing-reduced line strength factors $Z^2S_r$, vs. the reciprocal screened charge $1/(Z\text{-}2.757)$. Experimental measurements [7–17] and theoretical calculations [18] are denoted by (○) for the resonance transitions and by (×) for the intercombination transitions. Least squares fits to the experimental data are indicated by solid lines.

MCDF values (where they exist and experimental values do not), are given in Table I. The transition wavelength and empirical mixing angle factors were obtained from the observed spectroscopic energy level data which are given in Refs. [19–22] and extend through $4 \leqslant Z \leqslant 42$. For extrapolations for $Z \geqslant 43$, the theoretical energy level calculations of Ref. [18] can be used.

The plot in Fig. 3 uses the abscissa $1/(Z - 2.757)$, which was chosen to minimize deviations from linearity in the fit to the experimental data for the resonance transition. Weighted least squares adjustments of the parameters in eq. (2) were made to fit the experimental data, and these fits are indicated by solid lines. The weights were constructed from the quoted experimental uncertainties. In cases where multiple measurements for the same ion are available, the most recent or the most accurate result has been selected. Two lifetime measurements (in Si and Cl) for the resonance transition were far off the trend, and were excluded from our data set (cf discussion in Ref. [3]). The intercombination lifetime for Fe [15] was similarly far from the trend, and was excluded from the fit and plot, although it is included in Table I. Theoretical results for high $Z$ were also plotted in Fig. 3, but only for the purpose of qualitatively examining the possible breakdown of these linearities at high $Z$. Theoretical values were not included in the fit.

The theoretical results reduced in this manner exhibit a small $S$-curvature at high $Z$, with a small hump near $Z = 60$ followed by a slight downturn after $Z = 70$. New lifetime measurements would be required to determine whether this curvature is physical or an artifact of the calculation (curiously, semiempirical reductions often reveal a more nearly linear behaviour for measured data than for *ab initio* calculations, cf Ref. [23]). These curvatures are relatively small, and do not greatly deviate from the linear approximation.

The fit of eq. (2) to the reduced measured lifetimes of the resonance transition yielded the values $A = 39.128$, $B = 157.59$ and $C = 2.757$. The same value of $C$ was used for the

Table I. *Beryllium isoelectronic sequence. Experimental and theoretical lifetimes for the $2s2p\ ^3P_1'$ levels are compared to predictions made by least squares fits of eq. (2) to the mixing-reduced line strength values $Z^2S_r$ formed from the experimental results. Lifetimes are in seconds, theoretical values are in parentheses and for experimental measurements, A(B)E-C [D] denotes a value $A \times 10^{-C}$ with uncertainty B in the last decimal place and source reference [D]*

| | Intercombination τ(s) | | Resonance τ(s) | |
|---|---|---|---|---|
| Z | Pred[a] | Obs (Unc) [Ref] or (MCDF)[c] | Pred[b] | Obs (Unc) [Ref] or (MCDF)[c] |
| 4 | 6.59E−0 | | 1.85E−9 | 1.85(7)E−9 [7] |
| 5 | 1.59E−1 | | 8.56E−10 | 8.60(70)E−10 [8] |
| 6 | 1.30E−2 | 1.33(36)E−2 [14] | 5.67E−10 | 5.70(20)E−10 [9] |
| 7 | 2.15E−3 | (2.13E−3)[c] | 4.26E−10 | 4.25(15)E−10 [10] |
| 8 | 5.17E−4 | (5.19E−4)[c] | 3.42E−10 | 3.38(15)E−10 [10] |
| 9 | 1.58E−4 | (1.63E−4)[c] | 2.86E−10 | (2.48E−10)[c] |
| 10 | 5.71E−5 | (5.93E−5)[c] | 2.45E−10 | 2.32(37)E−10 [11] |
| 11 | 2.36E−5 | (2.47E−5)[c] | 2.14E−10 | (1.92E−10)[c] |
| 12 | 1.08E−5 | (1.14E−5)[c] | 1.89E−10 | 1.90(15)E−10 [12] |
| 13 | 5.31E−6 | (5.64E−6)[c] | 1.69E−10 | 1.75(15)E−10 [12] |
| 14 | 2.80E−6 | (2.98E−6)[c] | 1.52E−10 | 1.50(12)E−10 [12] |
| 15 | 1.55E−6 | (1.66E−6)[c] | 1.38E−10 | 1.40(10)E−10 [12] |
| 16 | 8.95E−7 | (9.66E−7)[c] | 1.26E−10 | 1.30(15)E−10 [12] |
| 17 | 5.40E−7 | (5.84E−7)[c] | 1.15E−10 | (1.08E−10)[c] |
| 18 | 3.38E−7 | (3.65E−7)[c] | 1.05E−10 | (9.91E−11)[c] |
| 19 | 2.19E−7 | (2.35E−7)[c] | 9.64E−11 | (9.11E−11)[c] |
| 20 | 1.44E−7 | (1.55E−7)[c] | 8.85E−11 | (8.37E−11)[c] |
| 21 | 9.75E−8 | (1.04E−7)[c] | 8.12E−11 | (7.69E−11)[c] |
| 22 | 6.78E−8 | (7.29E−8)[c] | 7.46E−11 | (7.06E−11)[c] |
| 23 | 4.79E−8 | (5.16E−8)[c] | 6.84E−11 | (6.48E−11)[c] |
| 24 | 3.45E−8 | (3.72E−8)[c] | 6.27E−11 | (5.94E−11)[c] |
| 25 | 2.54E−8 | (2.73E−8)[c] | 5.74E−11 | (5.43E−11)[c] |
| 26 | 1.90E−8 | 1.30(40)E−8 [15][x] | 5.25E−11 | 5.10(50)E−11 [13] |
| 27 | 1.45E−8 | (1.55E−8)[c] | 4.78E−11 | (4.51E−11)[c] |
| 28 | 1.12E−8 | (1.20E−8)[c] | 4.36E−11 | (4.10E−11)[c] |
| 29 | 8.82E−9 | (9.37E−9)[c] | 3.96E−11 | (3.72E−11)[c] |
| 30 | 7.04E−9 | (7.45E−9)[c] | 3.59E−11 | (3.36E−11)[c] |
| 31 | 5.69E−9 | | 3.24E−11 | |
| 32 | 4.67E−9 | | 2.92E−11 | |
| 33 | 3.88E−9 | | 2.63E−11 | |
| 34 | 3.26E−9 | | 2.35E−11 | |
| 35 | 2.77E−9 | (2.89E−9)[c] | 2.10E−11 | (1.94E−11)[c] |
| 36 | 2.38E−9 | 2.30(30)E−9 [16] | 1.88E−11 | (1.72E−11)[c] |
| 37 | 2.07E−9 | | 1.66E−11 | |
| 38 | 1.81E−9 | | 1.47E−11 | |
| 39 | 1.60E−9 | | 1.30E−11 | |
| 40 | 1.43E−9 | | 1.14E−11 | |
| 41 | 1.28E−9 | (1.31E−9)[c] | 1.01E−11 | (9.15E−12)[c] |
| 42 | 1.15E−9 | (1.18E−9)[c] | 8.86E−12 | (8.00E−12)[c] |
| 43 | 1.04E−9 | | 7.78E−12 | |
| 44 | 9.44E−10 | | 6.83E−12 | |
| 45 | 8.64E−10 | | 5.98E−12 | |
| 46 | 7.93E−10 | | 5.22E−12 | |
| 47 | 7.31E−10 | | 4.55E−12 | |
| 48 | 6.76E−10 | (7.03E−10)[c] | 3.96E−12 | (3.48E−12)[c] |
| 49 | 6.28E−10 | | 3.44E−12 | |
| 50 | 5.85E−10 | | 2.99E−12 | |
| 51 | 5.46E−10 | | 2.60E−12 | |
| 52 | 5.11E−10 | | 2.26E−12 | |
| 53 | 4.80E−10 | (5.05E−10)[c] | 1.96E−12 | (1.69E−12)[c] |
| 54 | 4.51E−10 | 4.7(5)E−10 [17] | 1.70E−12 | (1.47E−12)[c] |
| 59 | 3.40E−10 | (3.65E−10)[c] | 8.30E−13 | (7.11E−13)[c] |
| 64 | 2.63E−10 | (2.88E−10)[c] | 4.07E−13 | (3.48E−13)[c] |
| 69 | 2.07E−10 | (2.33E−10)[c] | 2.02E−13 | (1.73E−13)[c] |
| 74 | 1.65E−10 | (1.91E−10)[c] | 1.01E−13 | (8.71E−14)[c] |
| 79 | 1.33E−10 | (1.58E−10)[c] | 5.14E−14 | (4.48E−14)[c] |
| 80 | 1.27E−10 | (1.53E−10)[c] | 4.50E−14 | (3.93E−14)[c] |
| 82 | 1.17E−10 | (1.43E−10)[c] | 3.45E−14 | (3.03E−14)[c] |
| 92 | 8.02E−11 | (1.07E−10)[c] | 9.39E−15 | (8.61E−15)[c] |

[a] Eqs. (1, 2, 4, 5, 8, 9), using $A = 36.495$, $B = 43.18$, $C = 2.757$
[b] Eqs. (1, 2, 4, 5, 8, 9), using $A = 39.128$, $B = 157.59$, $C = 2.757$
[c] MCDF calculation, Cheng, Kim and Desclaux, Ref. [18] (not used in fit).
[x] Excluded from the fit.

Table II. *Magnesium isoelectronic sequence. Experimental and theoretical lifetimes for the $3s3p\ ^3P_1'$ and $^1P_1'$ levels are compared to predictions made by least squares fits of eq. (2) to the mixing-reduced line strength values $Z^2S_r$ formed from the experimental results. Lifetimes are in seconds, theoretical values are in parentheses and for experimental measurements, A(B)E-C [D] denotes a value A × $10^{-C}$ with uncertainty B in the last decimal place and source reference [D]*

| Intercombination τ(s) | | | Resonance τ(s) | |
|---|---|---|---|---|
| Z | Pred[a] | Obs (Unc) [Ref] or (MCDF)[c] | Pred[b] | Obs (Unc) [Ref] or (MCDF)[c] |
| 12 | 2.56E−3 | 4.57(63)E−3 [31][b] | 2.00E−9 | 2.0(1)E−9 [24] |
| 13 | 2.82E−4 | 3.00(21)E−4 [32] | 7.24E−10 | 7.2(11)E−10 [25] |
| 14 | 5.99E−5 | 5.99(36)E−5 [33] | 4.10E−10 | 4.1(9)E−10 [26] |
| 15 | 1.81E−5 | | 2.75E−10 | |
| 16 | 6.72E−6 | | 2.02E−10 | 1.9(1)E−10 [27] |
| 17 | 2.88E−6 | (2.48E−6)[c] | 1.57E−10 | (1.54E−10)[c] |
| 18 | 1.37E−6 | | 1.27E−10 | 1.32(5)E−10 [28] |
| 19 | 7.05E−7 | | 1.06E−10 | |
| 20 | 3.85E−7 | (3.56E−7)[c] | 8.99E−11 | (9.07E−11)[c] |
| 21 | 2.24E−7 | | 7.75E−11 | |
| 22 | 1.35E−7 | | 6.77E−11 | |
| 23 | 8.45E−8 | | 5.98E−11 | |
| 24 | 5.47E−8 | | 5.32E−11 | |
| 25 | 3.64E−8 | | 4.76E−11 | |
| 26 | 2.50E−8 | 2.60(26)E−8 [34] | 4.29E−11 | 4.2(3)E−11 [29] |
| 27 | 1.74E−8 | 1.75(15)E−8 [35] | 3.88E−11 | |
| 28 | 1.25E−8 | 1.20(10)E−8 [36] | 3.52E−11 | 3.1(6)E−11 [30] |
| 29 | 9.08E−9 | 8.80(60)E−8 [36] | 3.21E−11 | |
| 30 | 6.72E−9 | 6.95(50)E−8 [37] | 2.93E−11 | (3.13E−11)[c] |
| 31 | 5.07E−9 | | 2.68E−11 | |
| 32 | 3.88E−9 | | 2.45E−11 | |
| 33 | 3.03E−9 | | 2.25E−11 | |
| 34 | 2.39E−9 | | 2.06E−11 | |
| 35 | 1.91E−9 | | 1.89E−11 | |
| 36 | 1.54E−9 | (1.51E−9)[c] | 1.74E−11 | (1.89E−11)[c] |
| 37 | 1.26E−9 | | 1.60E−11 | |
| 38 | 1.05E−9 | | 1.47E−11 | |
| 39 | 8.78E−10 | | 1.35E−11 | |
| 40 | 7.43E−10 | | 1.23E−11 | |
| 41 | 6.37E−10 | | 1.13E−11 | |
| 42 | 5.49E−10 | (5.49E−10)[c] | 1.03E−11 | (1.14E−11)[c] |
| 47 | 2.91E−10 | | 6.51E−12 | |
| 48 | 2.62E−10 | (2.65E−10)[c] | 5.91E−12 | (6.50E−12)[c] |
| 54 | 1.53E−10 | (1.58E−10)[c] | 3.21E−12 | (3.54E−12)[c] |
| 64 | 8.06E−11 | (8.63E−11)[c] | 1.06E−12 | (1.18E−12)[c] |
| 74 | 4.98E−11 | (5.60E−11)[c] | 3.28E−13 | (3.70E−13)[c] |
| 79 | 4.04E−11 | | 1.81E−13 | |
| 80 | 3.88E−11 | | 1.60E−13 | |
| 82 | 3.58E−11 | (4.21E−11)[c] | 1.26E−13 | (1.45E−13)[c] |
| 92 | 2.48E−11 | (3.10E−11)[c] | 4.02E−14 | (4.64E−14)[c] |

[a] Eqs. (1, 2, 4, 5, 8, 9), using $A$ = 276.224, $B$ = 2071.21, $C$ = 10.533.
[b] Eqs. (1, 2, 4, 5, 8, 9), using $A$ = 335.934, $B$ = 3147.83, $C$ = 10.533.
[c] MCDF Calculation, Cheng and Johnson Ref. [38] (not used in fit).
[d] Excluded from the fit.

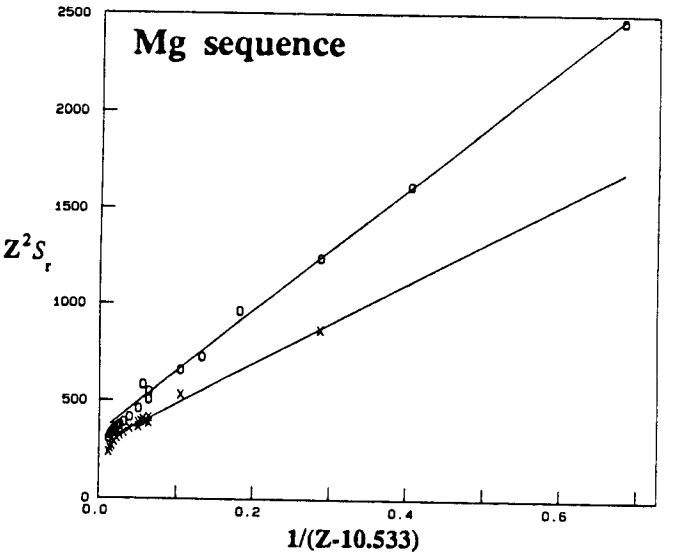


*Fig. 4.* Lifetimes for the $3s^2$–$3s3p$ resonance and intercombination transitions in the Mg sequence, converted to spin-mixing-reduced line strength factors $Z^2S_r$, vs. the reciprocal screened charge $1/(Z\text{-}10.533)$. Experimental measurements [24–37] and theoretical calculations [38] are denoted by (O) for the resonance transitions and by (×) for the intercombination transitions. Least squares fits to the experimental data are indicated by solid lines.

eighted least squares adjustment to the reduced measured fetime of the intercombination transition, which yielded = 36.495 and $B$ = 43.19. These fitting parameters were sed to generate mixing-reduced line strengths for all values f $Z$, and converted to lifetimes by appropriate wavelength nd mixing angle factors. Although the linearization of q. (2) is probably not rigorously valid at high $Z$, the slowly arying regularity exhibited by Fig. 3 is favourable to interolation and extrapolation. With a few new lifetime measurements extending to higher $Z$, it should be possible to generate highly accurate empirical predictions for the lifetimes of all ions in the isoelectronic sequence.

## 4. The Mg isoelectronic sequence

In a homologous manner, an exposition of the reduction of the $3s^2$–$3s3p$ resonance and intercombination transition lifetime data in the Mg sequence to the quantities $Z^2S_r$(Res) (denoted by 0) and $Z^2S_r$(Int) (denoted by X) is presented in Fig. 4. Here the measured lifetime data were obtained from Refs. [24–30] for the resonance lines and from Refs. [31–37] for the intercombination lines. Again here, the experimental lifetime data have been supplemented on the plot for high $Z$ by published MCDF theoretical calculations [38]. The measured lifetimes, their quoted uncertainties, and the MCDF values are given in Table II. The transition wavelength and empirical mixing angle factors were obtained from the observed spectroscopic energy level data which are given in Refs. [39–45] and include $12 \leqslant Z \leqslant 45$. The spectroscopic data can be extended for $46 \leqslant Z \leqslant 84$ using the theoretical energy level calculations of Ref. [46]. As can be seen from Fig. 2, the mixing angle approaches its $jj$ limit $\sin^2\theta_1 = 1/3$ at high $Z$ and can be extrapolated from $Z = 84$ to 92, as can the wavelength values.

In Fig. 3, the plot uses the abscissa $1/(Z - 10.533)$, which was chosen to minimize deviations from linearity in the fit to the experimental data for the resonance transition. Weighted least squares adjustments of the parameters in eq. (2) were made to fit the experimental data, and the fits are indicated by solid lines. The weights were constructed from the quoted experimental uncertainties. Measurements published prior to 1976 were of low accuracy and were not included in our data set. Two measurements of the resonance transition lifetime in phosphorus disagreed both from each other and from the isoelectronic trend, and were excluded. The intercombination lifetime in neutral Mg [31] was excluded from the fit and the

plot (but included in Table II) because the level has little singlet-triplet mixing ($\sin\theta_1 = 0.0022$), and the mixing reduction is thus very sensitive to small perturbations in the energy levels. Again here, the theoretical results were plotted for the purpose of qualitatively examining the possible breakdown of these linearities at high $Z$, and were not included in the fit. Here the theoretical values again exhibit a slight downturn for $Z \geqslant 70$, but do not greatly deviate from the linear approximation.

The fit to the measured resonance transition lifetimes yielded the values $A = 335.934$, $B = 3147.83$ and $C = 10.533$. The same value of $C$ was used for the weighted least squares adjustment to the intercombination transition lifetime, which yielded $A = 276.22$ and $B = 2071.21$. These fitting parameters were used to generate predicted mixing-reduced line strengths for all values of $Z$, and converted to lifetimes by appropriate wavelength and mixing angle factors. Here again the slowly varying regularity of the plot indicates that, if sufficient data were available, very accurate interpolative and extrapolative predictions could be made.

## 5. The Ne isoelectronic sequence

The $2p^6\ {}^1S_0$–$2p^5 3s\ {}^{1,3}P_1$ resonance and intercombination transitions in the Ne isoelectronic sequence are similar to the corresponding alkaline-earthlike transitions, but have two important distinctions. First, they involve $\Delta n = 1$ (rather than $\Delta n = 0$) transitions, hence at high $Z$ the transition energies are larger and the lifetimes are much shorter than those of the corresponding alkaline-earthlike systems. Second, the singlet-triplet mixing angles are much larger and have a complicated dependence upon $Z$. As can be seen from Fig. 2, $\theta_1$ first *decreases* from 15° to 12° between $Z = 10$ and 11, then increases sharply and passes through 45° (equal amplitudes of singlet and triplet) at $Z = 24$, and already by $Z = 40$ it is approaching the *jj* coupling limit of 54.7°. Thus, above $Z = 24$ the singlet-triplet characterizations of the physical states exchange roles, and at high $Z$ the eigenstate labelled "singlet" at the neutral end of the sequence is 67% triplet and *vice versa*.

These neonlike resonance and intercombination transitions are prominent in high temperature plasmas, and are important for diagnostic purposes in laser-produced and magnetically confined plasmas. However, direct measurements of the very short lifetimes of these levels are difficult for the higher ionization stages of this sequence. For lifetimes in the range between picoseconds and femtoseconds, the decay length is too short to be measured by time-of-flight methods and the natural linewidth is too narrow to be determined spectroscopically. Therefore, theoretical calculations and semiempirical extrapolations are especially important for this sequence.

The fact that the two $J = 1$ levels of the $2p^5\ 3s$ configuration have a mixing angle $\theta_1 > 45°$ for $Z \geqslant 24$ can cause two types of notational difficulties. The lesser of these is the choice among Paschen, $LS$ and $jj$ notations, which are only nominal for this sequence ($LS$ labels based on the dominant low $Z$ configuration have been used here only for compactness). A more serious problem concerns the choice between labelling the eigenvectors and labelling the energy levels. The eigenvectors are monotonic functions of $\theta_1$ which cross at $Z = 24$, whereas interacting levels of the same $J$ and parity $\Pi$ do not cross, but instead exchange eigenvector constituencies at an avoided crossing at $Z = 24$. (A discussion of notational difficulties in the presence of avoided crossings is presented in Ref. [47].) Although data compilations tend to present levels of the same $J$ and $\Pi$ labelled by their energy ordering, when isoelectronic sequences are interpolated and extrapolated it is essential that the correct eigenvectors be traced through an avoided crossing. Thus the transition we shall here call the "resonance line" has the *shorter* wavelength and lifetime at *low* $Z$ and the *longer* wavelength and lifetime at *high* $Z$. Similarly, the transition we call the "intercombination line" has the *longer* wavelength and lifetime at *low* $Z$ and the *shorter* wavelength and lifetime at *high* $Z$. In this context low $Z$ means $Z < 24$ and high $Z$ means $Z > 24$.

An exposition of the reduction of the $2p^6$–$2p^5 3s$ resonance and intercombination transition lifetime data in the Ne sequence to the quantities $Z^2S_r$(Res) and $Z^2S_r$(Int) is presented in Fig. 5. Lifetime measurements for these resonance and intercombination transitions are presently available for only a few ions in this sequence. The results of these measurements and their quoted uncertainties are given in Table III, and their sources are given in Refs. [48, 49]. Theoretical calculations for lifetimes in selected ions are available in, for example, Ref. [50], and these calculations are also listed in Table III. A number of high precision wavelength studies have been carried out in the past four years, and spectroscopic classifications and energy level data now exist for most ions for $10 \leqslant Z \leqslant 29$, given in Refs. [51–58]. Theoretical calculations for these energy levels are available for $20 \leqslant Z \leqslant 80$ in Ref. [59], which agree well with experiment in the region of overlap. As can be seen from Fig. 2, the values of $\sin^2\theta_1$ obtained from the experimental and theoretical energy level data connect smoothly between $Z = 29$ and 30 (although this mixing angle plot reveals a small inflection in the theoretical calculations between $Z = 53$ and 54 that is not evident from the energy level data directly). As can be seen from Fig. 2, the mixing angles saturate to the *jj* limit $\sin^2\theta_1 = 2/3$

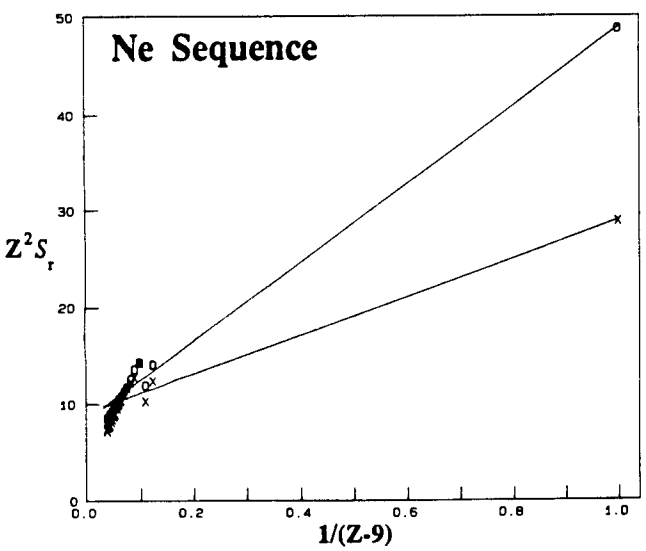


*Fig. 5.* Lifetimes for the $2p^6$–$2p^5 3s$ resonance and intercombination transitions in the Ne sequence, converted to spin-mixing-reduced line strength factors $Z^2S_r$, vs. the reciprocal screened charge $1/(Z\text{-}9)$. Experimental measurements [48, 49] and theoretical calculations [50] are denoted by (O) for the resonance transitions and by (x) for the intercombination transitions. Least squares fits to the experimental data are indicated by solid lines.

Table III. *Neon isoelectronic sequence. Experimental and theoretical lifetimes for the $2p^5 3s\ ^3P_1'$ and $^1P_1'$ levels are compared to predictions made by least squares fits of eq. (2) to the mixing-reduced line strength values $Z^2S_r$ formed from the experimental results. Lifetimes are in seconds, theoretical values are in parentheses and for experimental measurements, A(B)E-C [D] denotes a value $A \times 10^{-C}$ with uncertainty B in the last decimal place and source reference [D]*

| | Intercombination τ(s) | | Resonance τ(s) | |
|---|---|---|---|---|
| Z | Pred[a] | Obs (Unc) [Ref] or (HFR)[c] | Pred[b] | Obs (Unc) [Ref] or (HFR)[c] |
| 10 | 2.98E−8 | 2.98(20)E−8 [48] | 1.30E−9 | 1.3(1)E−9 [48] |
| 11 | 1.10E−8 | | 3.38E−10 | |
| 12 | 3.30E−9 | | 1.28E−10 | |
| 13 | 1.05E−9 | | 5.99E−11 | |
| 14 | 3.72E−10 | | 3.21E−11 | |
| 15 | 1.88E−10 | | 1.85E−11 | |
| 16 | 6.56E−11 | | 1.23E−11 | |
| 17 | 3.23E−11 | 3.0(5)E−11 [49] | 8.45E−12 | 8.0(2)E−12 [49] |
| 18 | 1.74E−11 | 1.9(4)E−11 [49] | 6.09E−12 | 6.5(20)E−12 [49] |
| 19 | 1.01E−11 | (7.80E−12)[c] | 4.56E−12 | (3.98E−12) |
| 20 | 6.33E−12 | (5.17E−12)[c] | 3.50E−12 | (3.18E−12) |
| 21 | 4.19E−12 | (3.60E−12)[c] | 2.74E−12 | (2.58E−12) |
| 22 | 2.88E−12 | (2.61E−12)[c] | 2.18E−12 | (2.13E−12) |
| 23 | 2.06E−12 | (1.95E−12)[c] | 1.76E−12 | (1.76E−12) |
| 24 | 1.46E−12 | (1.45E−12)[c] | 1.49E−12 | (1.52E−12) |
| 25 | 1.10E−12 | (1.14E−12)[c] | 1.23E−12 | (1.28E−12)[c] |
| 26 | 8.45E−13 | (9.06E−13)[c] | 1.02E−12 | (1.08E−12)[c] |
| 27 | 6.60E−13 | (7.33E−13)[c] | 8.49E−13 | (9.22E−13)[c] |
| 28 | 5.22E−13 | (6.01E−13)[c] | 7.18E−13 | (7.88E−13)[c] |
| 29 | 4.21E−13 | (4.98E−13)[c] | 6.06E−13 | (6.77E−13)[c] |
| 30 | 3.44E−13 | (4.17E−13)[c] | 5.15E−13 | (5.83E−13)[c] |
| 31 | 2.83E−13 | (3.52E−13)[c] | 4.41E−13 | (5.04E−13)[c] |
| 32 | 2.34E−13 | (3.00E−13)[c] | 3.81E−13 | (4.38E−13)[c] |
| 33 | 1.96E−13 | (2.57E−13)[c] | 3.30E−13 | (3.81E−13)[c] |
| 34 | 1.65E−13 | (2.22E−13)[c] | 2.87E−13 | (3.32E−13)[c] |
| 35 | 1.40E−13 | | 2.50E−13 | |
| 36 | 1.20E−13 | | 2.20E−13 | |
| 37 | 1.03E−13 | | 1.93E−13 | |
| 38 | 8.90E−14 | | 1.71E−13 | |
| 39 | 7.73E−14 | | 1.51E−13 | |
| 40 | 6.74E−14 | | 1.34E−13 | |
| 41 | 5.90E−14 | | 1.20E−13 | |
| 42 | 5.18E−14 | | 1.07E−13 | |
| 47 | 2.87E−14 | | 6.42E−14 | |
| 54 | 1.39E−14 | | 3.47E−14 | |
| 74 | 2.78E−15 | | 9.11E−15 | |
| 79 | 1.97E−15 | | 7.05E−15 | |
| 80 | 1.84E−15 | | 6.72E−15 | |
| 82 | 1.62E−15 | | 6.12E−15 | |
| 92 | 9.34E−16 | (2.3E−15)[d] | 4.30E−15 | (8.28E−15)[c] |

[a] Eqs. (1, 2, 4, 5, 8, 9) with $A = 9.1002$ $B = 19.894$, $C = 9$
[b] Eqs. (1, 2, 4, 5, 8, 9) with $A = 8.3472$, $B = 40.496$, $C = 9$
[c] HFR calculation of Biemont and Hansen [50] (not used in fit)
[d] Single configuration Dirac-Fock calculation using the program MCDF [60].

arly in the sequence, and can be easily extrapolated from $Z = 80$ to 92, as can the wavelengths.

In Fig. 5, the plot uses the abscissa $1/(Z\text{-}9)$, the reciprocal creened charge in the limit of total screening by the core lectrons. In this case there are only three experimental points n each of the isoelectronic trajectories, two of which are at djacent $Z$ values. Thus no attempt was made to optimize the nearity of the plot by adjusting $C$. With this value fixed at $= 9$, weighted least squares adjustments of the other parameters in eq. (2) were made to fit the experimental data, and the fits are indicated by solid lines. As before, weights were constructed from the quoted experimental uncertainties, and no theoretical values were included in the fit.

Notice that, while the standard resonance and intercombination line strength factors $Z^2S$ would undergo a crossing (or, depending on labelling, an avoided crossing) at $Z = 24$, the linear fits to the mixing-reduced line strengths $Z^2S_r$ converge toward a crossing at a much higher value of $Z$. This illustrates that the $Z = 24$ eigenvector crossing arises entirely from intermediate coupling, and is not exhibited by the radial transition moments that remain in eqs. (6, 7) after the mixing angle dependence has been removed.

When presented on this plot the theoretical values of Ref. [50] are also very nearly linear, but have a steeper slope than the experimental values, although their magnitudes are commensurate. Since there is yet no overlap of these theoretical values with experiment, it is not clear whether this difference in slope indicates a downturn from the linearity as seen in Figs. 3 and 4, or a discrepancy in values. The use of the mixing angle reduction also removes the $Z = 24$ crossing from the theoretical reduced line strengths.

The fits yielded the values $A = 8.342$ and $B = 40.50$ for the reduced lifetimes of the resonance transition and the values $A = 9.100$ and $B = 19.89$ for the reduced lifetimes of the intercombination transition. These fitting parameters were used to generate predicted mixing-reduced line strengths for all values of $Z$, and converted to lifetimes by appropriate wavelength and mixing angle factors. A theoretical value for $Z = 92$ was obtained by performing a single configuration Dirac–Fock calculation, using the program MCDF [60]. Although the experimental lifetime data for this sequence are sparse, there is some indication in Fig. 5 that, when additional measurements become available, accurate interpolative and extrapolative predictions should be possible using this formalism.

## 6. Conclusions

The method described here can utilize a few well-chosen lifetime measurements together with comprehensive energy level data to predict a level lifetime for all ions in an isoelectronic sequence. The accuracy of the method is dependent on the quantity and precision of the available data base, but the results obtained here indicate that a relatively small number of precision lifetime measurements at separated values of $Z$ should be sufficient for these sequences. This method is also directly applicable to higher homologous sequences, e.g., to the $4s^2$–$4s4p$ transitions in the Zn sequence and $3p^6$–$3p^5 4s$ and $4p^6$–$4p^5 5s$ transitions in the Ar and Kr sequences. A decay branched version of the method could be used to study levels of higher principal quantum number, e.g., the $2s^2$–$2s3p$ transitions in the Be sequence and the $3s^2$–$3s4p$ transitions in the Mg sequence. Despite the multiply branched decay of these upper levels, experimental determinations of their intercombination transition rates have been made by a technique employing differential lifetime measurements [61–63]. These higher lying states are much more likely to be affected by configuration interaction [63] and cancellations in the transition moment [64], which could be investigated in this manner. The isoelectronic behaviour of these systems might be clarified by the mixing angle exposition,

which can separate intermediate coupling effects from other interactions.

## Acknowledgements

The author gratefully acknowledges the hospitality extended to him during his 1989–90 Sabbatical Leave at the University of Lund. This work was supported by the US Department of Energy, Office of Basic Energy Sciences, Division of Chemical Sciences, under grant number DE-FG05-88ER13958, by the Nordic Institute for Theoretical Atomic Physics (NORDITA), and by the Kungliga Fysiografiska Sällskapet of Lund.

## References

1. Edlén, B., Physica Scripta **17**, 565 (1978).
2. Reistad, N. and Martinson, I., Phys. Rev. **A34**, 2632 (1986).
3. Träbert, E., Z. Phys. **D9**, 143 (1988).
4. Theodosiou, C. E., and Curtis, L. J., Phys. Rev. **A38**, 4435 (1988).
5. Kim, Y.-K. and Cheng, K.-T., J. Opt. Soc. Am. **68**, 836 (1978).
6. Curtis, L. J., Phys. Rev. **A40**, 6958 (1989).
7. Martinson, I., Gaupp, A. and Curtis, L. J., J. Phys. **B7**, L463 (1974).
8. Bashkin, S., McIntyre, L. C., v. Buttlar, H., Ekberg, J. O. and Martinson, I., Nucl. Instr. Meth. in Phys. Res. **B9**, 593 (1985).
9. Reistad, N., Hutton, R., Nilsson, A. E., Martinson, I. and Mannervik, S., Physica Scripta **34**, 151 (1986).
10. Engström, L., Denne, B., Ekberg, J. O., Jones, K. W., Jupén, C., Litzén, U., Meng, W. T., Trigueiros, A. and Martinson, I., Physica Scripta **24**, 551 (1981).
11. Irwin, D. J. G., Livingston, A. E. and Kernahan, J. A., Can. J. Phys. **51**, 1948 (1973).
12. Träbert, E. and Heckmann, P. H., Physica Scripta **22**, 489 (1980).
13. Buchet, J. P., Buchet-Poulizac, M. C., Denis, A., Désesquelles, J., Druetta, M., Grandin, J. P., Huet, M., Husson, X. and Lecler, D., Phys. Rev. **A30**, 309 (1984).
14. Smith, P. L., Johnson, B. C., Kwong, H. S. and Parkinson, W. H., Physica Scripta **T8**, 88 (1984).
15. Dietrich, D. D., Leavitt, J. A., Bashkin, S., Conway, J. G., Gould, H., MacDonald, D., Marrus, R., Johnson, B. M. and Pegg, D. J., Phys. Rev. **A18**, 208 (1978).
16. Dietrich, D. D., Leavitt, J. A., Gould, H. and Marrus, R., Phys. Rev. **A22**, 1109 (1980).
17. Möller, G., Träbert, E., V. Lodwig, V., Wagner, C., Heckmann, P. H., Blanke, J. H., Livingston, A. E. and Mokler, P. H., Z. Physik **D11**, 333 (1989).
18. Cheng, K.-T., Kim, Y.-K. and Desclaux, J. P., Atomic Data Nucl. Data Tables **24**, 111 (1979).
19. Johansson, L., Arkiv Fysik **23**, 119 (1962).
20. Ölme, A., Physica Scripta **1**, 256 (1970).
21. Edlén, B., Physica Scripta **28**, 51 (1983).
22. Denne, B., Magyar, G. and Jacquinot, J., Phys. Rev. **A40**, 3702 (1989).
23. Curtis, L. J., Comments At. Mol. Phys. **16**, 1 (1985).
24. Liljeby, L., Lindgård, A., Mannervik, S., Veje, E. and Jelenkovic, B., Physica Scripta **21**, 805 (1980).
25. Kernahan, J. A., Pinnington, E. H., O'Neill, J. A., Brooks, R. L. and Donnelly, K. E., Physica Scripta **19**, 267 (1979).
26. Livingston, A. E., Dumont, P. D., Baudinet-Robinet, Y., Garnir, H. P., Biemont, E. and Grevesse, N., in "Beam-Foil Spectroscopy 1" (Edited by I. A. Sellin and D. J. Pegg), p. 339, Plenum, New York (1976).
27. Reistad, N., Jupén, C., Huldt, S., Engström, L. and Martinson, I., Physica Scripta **32**, 164 (1985).
28. Reistad, N., Engström, L. and Berry, H. G., Physica Scripta **34**, 158 (1986).
29. Hutton, R. Engström, L. and Träbert, E., Nucl. Instr. Meth. in Phys. Res. **B31**, 294 (1988).
30. Hutton, R., Reistad, N., Martinson, I., Träbert, E., Heckman, P. H., Blanke, J. H., Hellmann, H. M. and Hucke, R., Physica Scripta **35**, 300 (1987).
31. Kwong, H. S., Smith, P. L. and Parkinson, W. H., Phys. Rev. **A25**, 2629 (1982).
32. Johnson, B. C., Smith, P. L. and Parkinson, W. H., Astrophys. J. **308**, 1013 (1986).
33. Kwong, H. S., Johnson, B. C., Smith, P. L. and Parkinson, W. H., Phys. Rev. **A27**, 3040 (1983).
34. Träbert, E., Hutton, R., and Martinson, I., Z. Physik **D5**, 125 (1987).
35. Träbert, E., Heckmann, P. H., Hutton, R. and Martinson, I., J. Opt. Soc. Am. **5**, 2173 (1988).
36. Träbert, E., Reistad, N. and Hutton, R., Z. Physik **D1**, 331 (1986).
37. Träbert, E., Heckmann, P. H. and Wiese, W. L., Z. Physik **D8**, 209 (1988).
38. Cheng, K.-T. and Johnson, W. R., Phys. Rev. **A16**, 263 (1977).
39. Curtis, L. J. and Ramanujam, P. S., J. Opt. Soc. Am. **73**, 979 (1983).
40. Jupén, C., Physica Scripta **36**, 776 (1987).
41. Litzén, U. and Redfors, A., Physica Scripta **36**, 895 (1987).
42. Sugar, J., Kaufman, V., Indelicato, P. and Rowan, W. L., J. Opt. Soc. Am. **B6**, 1437 (1989).
43. Ekberg, J. O., Feldman, U., Seely, J. F. and Brown, C. M., Physica Scripta **40**, 643 (1989).
44. Seely, J. F., Ekberg, J. O., Feldman, U., Schwob, J. L., Suckewer, S. and Wouters, A., J. Opt. Soc. Am. **B5**, 602 (1988).
45. Sugar, J., Kaufman, V. and Rowan, W. L., J. Opt. Soc. Am. **B4**, 1927 (1987).
46. Ivanova, E. P., Ivanov, L. N. and Tsirekidze, M. A., Atomic Data Nucl. Data Tables **35**, 419 (1986).
47. Maniak, S. T. and Curtis, L. J., Phys. Rev. **A42**, 1821 (1990).
48. Kernahan, J. A., Denis, A. and Drouin, R., Physica Scripta **4**, 49 (1971).
49. Berry, H. G., Désesquelles, J., Cheng, K.-T. and Schectman, R. M., Phys. Rev. **A18**, 546 (1978).
50. Biémont, E. and Hansen, J. E., Atom. Data Nucl. Data Tables **37**, 1 (1987).
51. Edlén, B., as compiled by Moore, C. E., in "Atomic Energy Levels Vol. I," NSRDS-NBS 35. US Gov. Printing Office, Washington DC (1948).
52. Martin, W. C. and Zalubas, R., J. Phys. Chem Ref. Data **10**, 153 (1981).
53. Jupén, C. (personal communication).
54. Jupén, C., Physica Scripta **36**, 776 (1987).
55. Engström, L. and Berry, H. G., Physica Scripta **34**, 131 (1986).
56. Gayazov, R. R., Kramida, A. E., Podobedova, L. I., Ragozin, E. N. and Chirkov, V. A., in "X-Ray Plasma Spectroscopy and Properties of Multiply Charged Ions", (Edited by I. I. Sobelman), p. 79, Nova Science Publ, USSR, (1988).
57. Jupén, C., Litzén, U., Kaufman, V. and Sugar, J., Phys. Rev. **A35**, 116 (1987).
58. Buchet, J. P., Buchet-Poulizac, M. C., Denis, A., Désesquelles, J., Druetta, M., Martin, S. and Wyart, J.-F., J. Phys. **B20**, 1709 (1987).
59. Ivanova, E. P. and Glushkov, A. V., J. Quant. Spectrosc. Radiat. Transfer **36**, 127 (1986).
60. Grant, I. P., McKenzie, B. J., Norrington, P. H., Mayers, D. F. and Pyper, N. C., Comput. Phys. Commun. **21**, 207 (1980); Dyall, K. G., Grant, I. P., Johnson, C. T., Parpia, F. A. and Plummer, E. P., *ibid.* **55**, 425 (1989).
61. Engström, L., Denne, B., Huldt, S., Ekberg, J. O., Curtis, L. J., Veje, E. and Martinson, I., Physica Scripta **20**, 88 (1979).
62. Hardis, J. E., Curtis, L. J., Ramanujam, P. S., Livingston, A. E. and Brooks, R. L., Phys. Rev. **A27**, 257 (1983).
63. Reistad, N., Brage, T., Ekberg, J. O. and Engström, L., Physica Scripta **30**, 249 (1984).
64. Curtis, L. J. and Ellis, D. G., J. Phys. **B11**, L543 (1978).